Volume 37
Number 1
January 2022
Pages 1–204

JAAS

Journal of Analytical Atomic Spectrometry

rsc.li/jaas

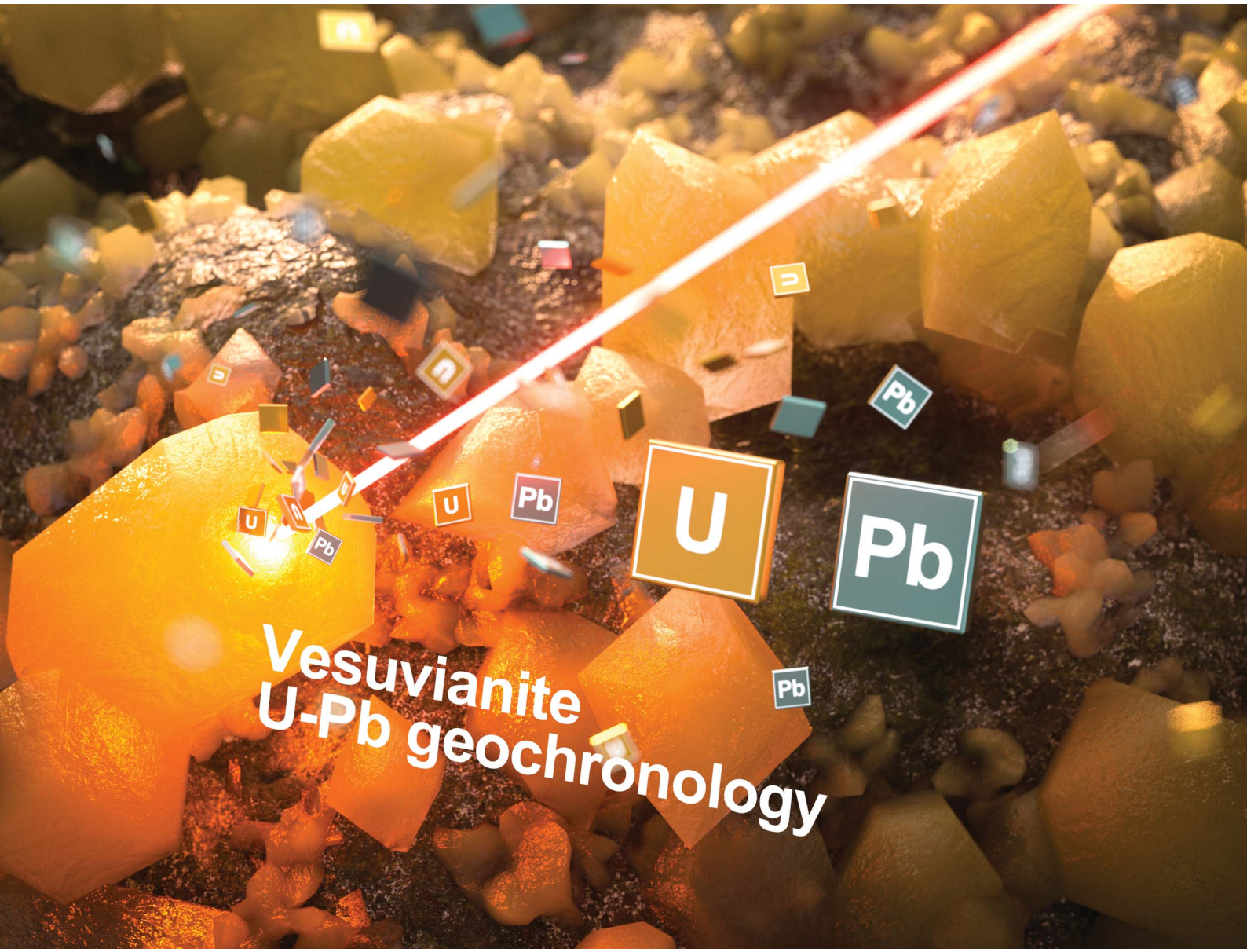

ISSN 0267-9477

ROYAL SOCIETY OF CHEMISTRY

COMMUNICATION

Yue-Heng Yang *et al.*

In situ U–Pb geochronology of vesuvianite by LA-SF-ICP-MS

JAAS

COMMUNICATION

View Article Online
View Journal | View Issue

Cite this: *J. Anal. At. Spectrom.*, 2022, **37**, 69

Received 30th August 2021
Accepted 8th November 2021

DOI: 10.1039/d1ja00303h

rsc.li/jaas

In situ U–Pb geochronology of vesuvianite by LA-SF-ICP-MS†

Qin-Di Wei,[abc] Ming Yang,[abc] Rolf L. Romer,[d] Hao Wang,[abc] Yue-Heng Yang,*[abc] Zi-Fu Zhao,[e] Shi-Tou Wu,[ab] Lie-Wen Xie,[ab] Chao Huang,[ab] Lei Xu,[ab] Jin-Hui Yang[abc] and Fu-Yuan Wu[abc]

We present a new procedure for U–Pb dating of vesuvianite using laser ablation sector field inductively coupled plasma mass spectrometry (LA-SF-ICP-MS). Vesuvianite is a common mineral in skarn ore deposits and in metamorphic and metasomatic argillaceous carbonate rocks. The age of vesuvianite growth directly dates the formation of skarn mineralization, possibly also the metamorphism and metasomatism of argillaceous limestones. Vesuvianite U–Pb dating may provide age information for hydrothermal, metamorphic, and metasomatic processes that may be hard to get by zircon U–Pb dating. We analyzed eleven vesuvianite samples. Matrix effects were corrected by using Ti-bearing andradite (schorlomite) of known age as no well-characterized vesuvianite was available as a U–Pb reference material. The robustness of the analytical protocol was assessed by additional U–Pb dating of four vesuvianite samples by ID-TIMS. The U–Pb ages determined by ID-TIMS and LA-SF-ICP-MS agree well within uncertainties. An additional seven vesuvianite samples yielded *in situ* U–Pb ages that agree with previously published zircon, cassiterite, or wolframite U–Pb ages from the same area. Therefore, U–Pb dating of vesuvianite by LA-SF-ICP-MS represents a fast, relatively low-cost approach with high spatial resolution that may be particularly suited to date skarn mineralization.

1. Introduction

Vesuvianite or idocrase ($(Ca, Na)_{19}(Al, Mg, Fe)_{13}(SiO_4)_{10}(Si_2O_7)_4(OH, F, O)_{10}$), as a common mineral, usually occurs in skarn ore deposits and in metamorphic and metasomatic argillaceous carbonate rocks.[1,2] Vesuvianite may have concentrations of several tens or hundreds ppm of U, but does not have particularly high $^{238}U/^{204}Pb$ as significant amounts of common Pb may substitute for Ca in this Ca-rich mineral.[3] The suitability of vesuvianite for U–Pb dating depends mainly on the age and the $^{238}U/^{204}Pb$ ratio of the mineral. The $^{238}U/^{204}Pb$ ratio depends on the availability of U in the rock and the presence of minerals that incorporate available Pb to a higher extent than vesuvianite does. There are few examples of successful Pb–Pb or U–Pb vesuvianite age determination by isotope dilution thermal ionization mass spectrometry (ID-TIMS),[3,4] although a great number of studies characterized the mineralogy and trace elemental geochemistry of vesuvianite.[5–11]

Romer[3] demonstrated that vesuvianite could yield directly the age of skarn ore deposits. Romer[3] presented an ID-TIMS U–Pb age of 1780 ± 9 Ma for a vesuvianite specimen from an early Proterozoic tungsten skarn mineral deposit at Björntjärn, northern Sweden. Romer and Heinrich[4] reported the ID-TIMS $^{206}Pb/^{238}U$ age of a 31.6 ± 0.3 Ma old idiomorphic vesuvianite crystal from the contact metamorphic aureole of the Bufa del Diente syenite intrusion, north-east Mexico. These vesuvianite crystals formed when magmatic aqueous fluids infiltrated the impure carbonate country rocks. Therefore, U–Pb dating of vesuvianite could provide the age of skarn deposits or of metamorphic and metasomatic alterations.

The high precision of ID-TIMS U–Pb dating of vesuvianite minerals is offset by the delicate and time-consuming analytical protocol.[12–14] Furthermore, the U–Pb TIMS dating of hydrothermal vesuvianite may be affected by the presence of U and/or Pb bearing inclusions. For instance, minuscule inclusions of Pb-rich minerals (*e.g.*, epidote, calcite, sulfide minerals, scheelite) may overwhelm the Pb budget of vesuvianite with common Pb, resulting in low $^{238}U/^{204}Pb$ ratios, and eventually making U–Pb dating challenging or impossible. Similarly, inclusions of U-rich minerals (*e.g.*, titanite) may dominate the U–Pb system of the vesuvianite bulk sample resulting in a situation, where the U–Pb system of the inclusion determines the age of the bulk

[a]*State Key Laboratory of Lithospheric Evolution, Institute of Geology and Geophysics, Chinese Academy of Sciences, Beijing, 100029, China. E-mail: yangyueheng@mail.iggcas.ac.cn*

[b]*Innovation Academy of Earth Science, Chinese Academy of Sciences, Beijing, 100029, China*

[c]*College of Earth and Planetary Sciences, University of Chinese Academy of Sciences, Beijing, 100049, China*

[d]*GFZ German Research Centre for Geosciences, Telegrafenberg, Potsdam, 14473, Germany*

[e]*CAS Key Laboratory of Crust-Mantle Materials and Environments, School of Earth and Space Science, University of Science and Technology of China, Hefei, 230026, China*

† Electronic supplementary information (ESI) available. See DOI: 10.1039/d1ja00303h

sample. *In situ* U–Pb dating of vesuvianite using a laser or ion probe avoids many of these problems inherent to ID-TIMS dating that needs a larger sample size and, therefore, has limited spatial resolution.[15–18] *In situ* U–Pb dating enables inclusions or altered domains to be avoided and allows texturally different domains to be analysed separately. Furthermore, sample preparation is relatively simple and fast. For isotopic dating using a laser or ion probe, however, a well-characterized vesuvianite reference material is currently not available.

The main goal of this study is to establish a procedure for *in situ* U–Pb dating of vesuvianite by LA-SF-ICP-MS. In the absence of a suitable vesuvianite refence material, we used Ti-bearing andradite (schorlomite) of known age to correct for matrix effects. To test the robustness of the analytical protocol, four vesuvianite samples dated by LA-SF-ICP-MS were also dated by ID-TIMS.

2. Experimental

2.1 Sample preparation

Vesuvianite samples investigated in this work are museum specimens (M is the prefix of the sample number, M659, M660, M784, M1377, M1439, M6599, M6601, M6608 M6635; Institute of Geology and Geophysics, Chinese Academy of Sciences (IGGCAS), Beijing), and were bought from a mineral trader (Wilui specimens), or have been studied earlier (Bufa, Romer and Heinrich[4]). Most vesuvianite samples had relatively large grains (up to several millimeters). Grains without visible inclusions were selected by hand picking under a binocular microscope. Selected grains were embedded in a 1 inch epoxy mount, sectioned to expose their interiors, polished, and photographed. The grain mount was cleaned in 2% HNO_3 for several minutes prior to laser ablation analysis. The vesuvianite crystals are yellow, brown, brown-black, emerald green or purple with a metallic or bituminous luster. Compositional zoning was generally not observed in optical or BSE images. Based on initial trace element analysis using ICP-MS, three vesuvianite samples (Wilui, M784, and M6635) characterized by relatively high U contents, old U–Pb ages, or low common Pb contents were selected for U–Pb determination for conventional ID-TIMS analysis.

2.2 ID-TIMS

U–Pb dating of vesuvianite by ID-TIMS was done at GFZ German Research Centre for Geoscience, Potsdam, Germany. Vesuvianite samples were immersed in warm dilute nitric acid for 30 minutes to remove surface contamination and carbonates. Then, they were rinsed with distilled H_2O and acetone before weighing. Aliquots were spiked with a mixed ^{205}Pb–^{235}U tracer. The samples were dissolved in 40% HF on a hotplate at 160 °C for three days. All samples were dried to a precipitate, redissolved in 1 mol L^{-1} HNO_3, and dried at low temperature to convert fluorides to nitrates. Lead and U separation was adapted from the HBr–HCl ion-exchange chromatography described in Romer and Heinrich.[4] Due to the high B content of sample Wilui (Wiluite), the Pb separation was repeated to remove borate that was not completely removed during the first separation (borate seems to suppress Pb and U ionization). U and Pb were loaded with H_3PO_4 and silica gel on the same Re single filament. The isotopic ratios of U and Pb were measured using a Triton TIMS instrument operated in static or dynamic multi-collection mode, depending on signal intensity, using Faraday collectors and an ion counter. Lead was analyzed at 1200–1260 °C and U at 1360–1430 °C. Data reduction followed the procedures described by Schmid *et al.*[19] The initial $^{206}Pb/^{204}Pb$ and $^{207}Pb/^{204}Pb$ were estimated using the $^{206}Pb/^{204}Pb$ *vs.* $^{238}U/^{204}Pb$ diagram and the $^{207}Pb/^{204}Pb$ *vs.* $^{206}Pb/^{204}Pb$ diagram, respectively. The procedural blank for Pb and U is better than 15 pg and 1 pg, respectively. The data were plotted using Isoplot 3.0.[20]

2.3 *In situ* U–Pb reference material

A well-characterized reference material is essential for *in situ* U–Pb dating. There is no vesuvianite reference material available for microanalysis. To handle this deficiency, we selected a Ti-bearing andradite (schorlomite) from a wollastonite ijolite of the Prairie Lake carbonatite complex (Northwestern Ontario, Canada; Wu *et al.*[21]). Vesuvianite and grossular-andradite have similar major element compositions (Table 1S†) and, therefore, may show similar matrix effects. Fig. 1 shows elemental fractionation of schorlomite PL34 and vesuvianite M6635 during laser sampling. No obvious $^{238}U/^{206}Pb$ fractionation was observed between schorlomite and vesuvianite, which confirms the expectation. The schorlomite PL34 and vesuvianite sample M6635 data were acquired using the same spot size and repetition rate as 44 μm and 8 Hz, respectively. The temporal variation of the signal indicates that fractionation of the two materials is similar.

Schorlomite PL34 has negligible common Pb contents and its age is well-constrained. Therefore, it was used as an in-house primary reference material. The Prairie Lake complex is composed of carbonatite, ijolite, and potassic nepheline syenite.[21] Two baddeleyite samples from the carbonatite yield SIMS U–Pb ages of 1157.2 ± 2.3 Ma and 1158.2 ± 3.8 Ma, identical to the ID-TIMS U–Pb age of 1163.6 ± 3.6 Ma obtained for baddeleyite from ijolite. Apatite from the carbonatite yields the same U–Pb age of ~1160 Ma using ID-TIMS, SIMS and laser ablation techniques. These data indicate that the various rocks forming this complex were synchronously emplaced at about 1160 Ma.[21,22] Therefore, we use a Concordia age of ~1160 Ma for schorlomite PL34.

2.4 LA-SF-ICP-MS

In situ U–Pb isotope measurements were made using a single collector SF-ICP-MS (Element XR, ThermoFisher Scientific) and a 193 nm ArF excimer laser (Geolas HD, Coherent), located at IGGCAS. The detailed description of instrumentation can be found in Wu *et al.*[23] Helium and nitrogen were used as carrier gases through the ablation cell and mixed with argon downstream of the ablation cell. Daily optimization of instrumental performance with NIST SRM 612 involved maximising the signal relative to background intensity ratios for Pb, Th and U,

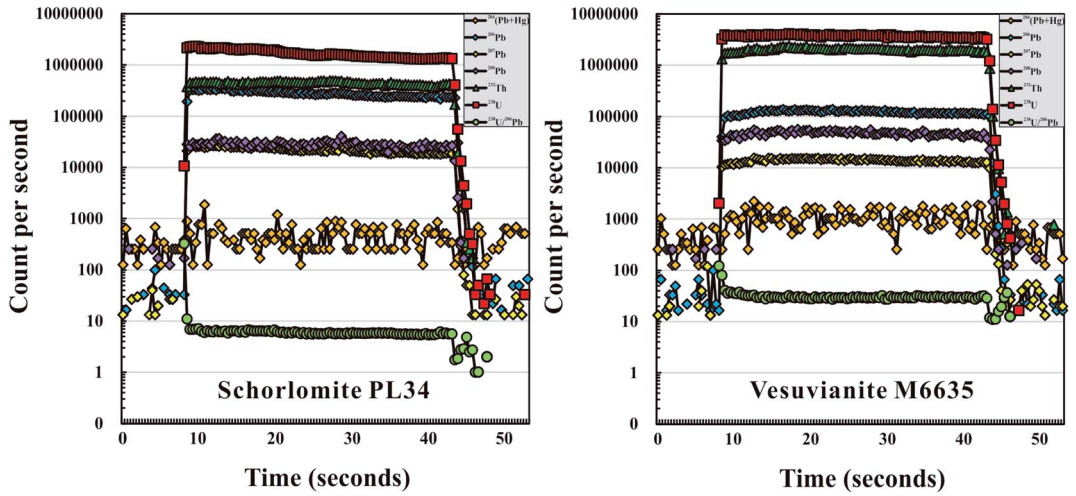

Fig. 1 Time *vs.* signal sensitivity of schorlomite PL34 and vesuvianite M6635 during typical LA-SF-ICP-MS analysis.

while satisfying low oxide production rates (ThO^+/Th^+ <0.5%), low double-charged ions (Ca^{2+}/Ca^+ <1.0%), and robust plasma conditions (U^+/Th^+ in a range of 0.95–1.05). The isotopes ^{202}Hg, ^{204}Pb, ^{206}Pb, ^{207}Pb, ^{208}Pb, ^{232}Th, ^{235}U, and ^{238}U were analyzed by cycling the electrostatic analyzer (EScan mode) at a static magnet mass. The dwell time was set to 15 ms for ^{206}Pb and ^{238}U, 2 ms for ^{202}Hg and ^{204}Pb, 10 ms for ^{208}Pb and ^{232}Th, and 30 ms for ^{207}Pb, respectively. Typical operating conditions are summarized in Table 1. We chose the 32, 44 or 60 μm diameter of ablation pit for precise analysis depending on the U content of vesuvianite samples. Each analytical session used the same spot size for the standard and samples. Prior to each analytical session, a pre-ablation run was used to remove any contamination from the vesuvianite surface by ablating a 90 μm spot for 2s. Each spot analysis consisted of an approximately 15 s background and 45 s sample data acquisition.

The raw data (the analytical sequence and the intensities for all isotopes of all analyses) were exported for offline data reduction using Iolite software for semi-quantitative calculation of trace element concentrations[24] and Glitter software for U–Pb age calculation.[25] Signals of ^{204}Pb, ^{206}Pb, ^{207}Pb, ^{208}Pb, ^{232}Th, and ^{238}U were acquired for U–Pb dating, whereas the ^{235}U signal was calculated from ^{238}U on the basis of the ratio $^{238}U/^{235}U = 137.818$.

The Ti-bearing andradite (schorlomite) PL34, used as a primary U–Pb reference material, showed systematic element fractionation allowing for downhole fractionation correction. To evaluate matrix effects, we also employed vesuvianite Wilui as an external calibration standard to calculate other vesuvianites. Vesuvianite samples M6635 and Bufa with known ID-TIMS U–Pb ages were used as secondary reference materials to monitor the reliability of our analytical protocol.

The mode of data reduction depended on the contribution of common Pb to the total amount of Pb present: samples with significant common Pb are reported as ages on a Tera–Wasserburg diagram. Weighted $^{206}Pb/^{238}U$ mean dates were calculated using the ^{207}Pb correction of common Pb,[26] assuming a common Pb composition corresponding to the two-stage crustal Pb model of Stacey and Kramers.[27] The U–Pb ages and weighted mean ages were calculated using the Isoplot 3.23 software package.[20]

Table 1 Typical LA-SF-ICP-MS instrumental parameters

Laser ablation system	
Manufacturer, model & type	Coherent, geolas HD
Ablation cell & volume	In-house built cell, aerosol dispersion volume <3 cm^3
Laser wavelength	193 nm
Pulse width	20 ns
Energy density/fluence	~4 J cm^{-2}
Repetition rate	5 Hz
Spot size	32, 44, 60 μm
Sampling mode/pattern	Single hole drilling, ten cleaning pulses
Ablation gas flow	~0.75 L min^{-1} (He)
Ablation duration	45 seconds
SF-ICP-MS	
Manufacturer, model & type	ThermoFisher scientific element XR
RF power	~1350 W
Guard electrode	Connected (pt)
Sample cone	Nickel Jet sample cone
Skimmer cone	Nickel "X" version skimmer cone
Coolant gas flow (ar)	15.00 L min^{-1}
Auxiliary gas flow (ar)	~0.80 L min^{-1}
Carrier gas flow (ar)	~0.94 L min^{-1}
Enhancement gas flow (N_2)	~5 mL min^{-1}
Scan mode	E-scan
Isotopes measured (m/z) + sample time	^{202}Hg (2 ms), ^{204}Pb (2 ms), ^{206}Pb (15 ms), ^{207}Pb (30 ms), ^{208}Pb (10 ms), ^{232}Th (10 ms), ^{235}U (10 ms), ^{238}U (15 ms)
Mass window	20%
Sample per peak	20
Detection system	Single SEM detector in triple mode, counting, analog and faraday
Resolution (M/ΔM)	Low (~300)
Total integration time per reading	0.27 s

3. Results and discussion

Chemical and isotopic homogeneities were assessed by reflected light together with the false-color backscattered electron (BSE) image (Fig. 2), electron probe microanalysis (EPMA) (Table S1†), and laser ablation sector field ICP-MS (LA-SF-ICP-MS) analyses. ID-TIMS U–Pb analytical results for vesuvianite are shown in Table 2. All age errors quoted in the text and in Table 2 and all error ellipses shown in concordia diagrams are given at 2s uncertainties. LA-SF-ICP-MS U–Pb results are summarized in Table 3. The individual U–Pb isotopic data of vesuvianite samples are provided in Table S2 in the ESI† (individual data of *in situ* U–Pb data).[28]

3.1 ID-TIMS U–Pb geochronology

Three vesuvianite samples (Wilui, M784, and M6635) were selected for ID-TIMS U–Pb analysis due to their relatively homogeneous LA-ICP-MS U–Pb ages and their low content of common Pb (Table 2). Wiluite vesuvianite is from the Vilyui and Akhtaragda Rivers, near Chernysheysk, Sakha-Yakutia, Russia. Seven aliquots of sample Wilui have been analyzed. The common Pb and U range from 0.1 to 0.5 μg g^{-1} and 11.6 to 17.4 μg g^{-1}, respectively (Table 2). The $^{206}Pb/^{204}Pb$ ratios of the individual fractions are relatively radiogenic and fall in the range of 422.6 to 638.3. In a $^{206}Pb/^{238}U$ *vs.* $^{207}Pb/^{235}U$ diagram, all Wilui vesuvianite analyses are concordant and overlap with each other. The apparent $^{206}Pb/^{238}U$ ages range from 254.9 ± 1.9

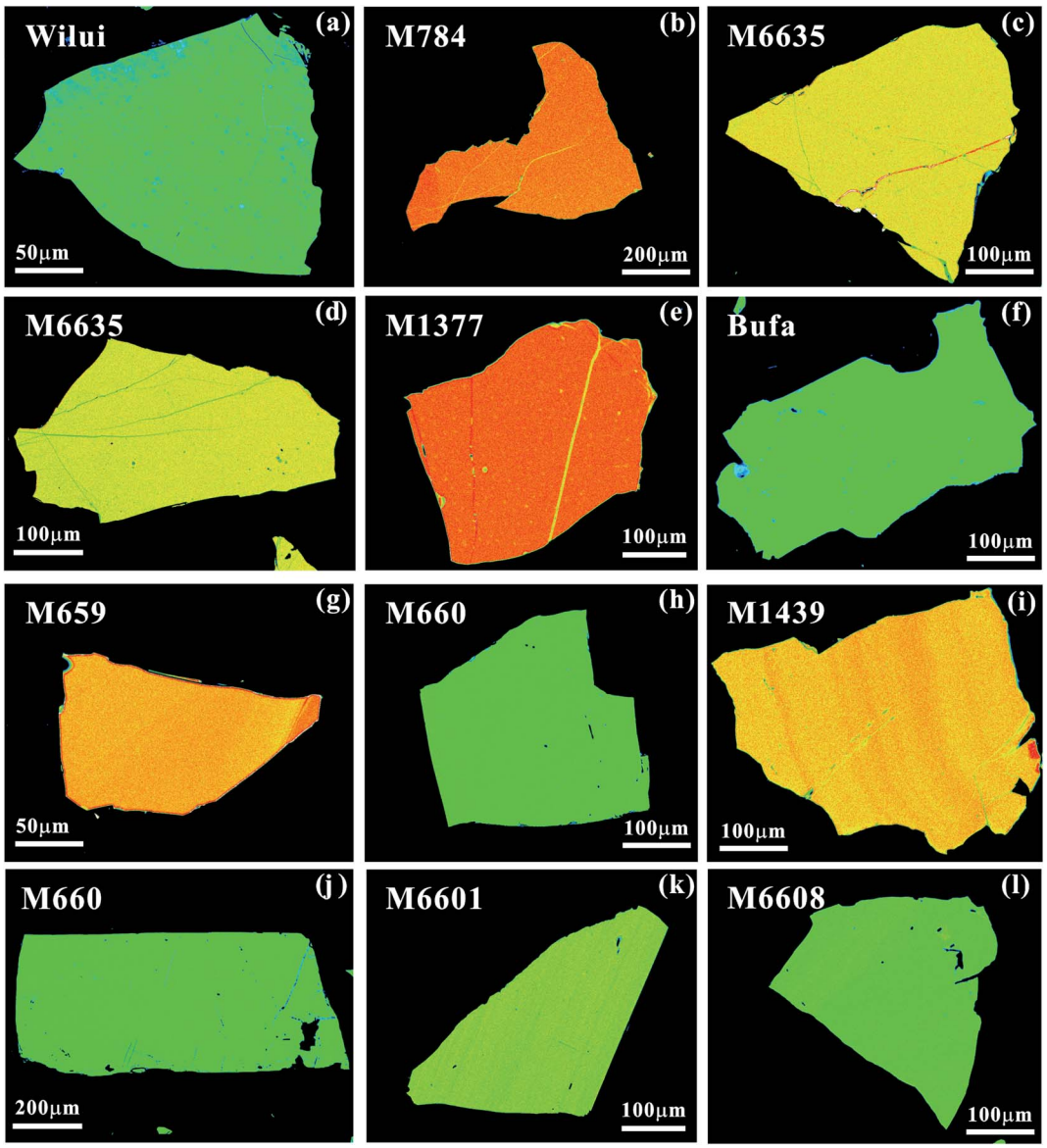

Fig. 2 False-color back-scattered electron (BSE) images of the investigated vesuvianite samples show no compositional zonation, with the exception of M659 and M1439. Some vesuvianite samples have healed fractures (clarification: false-color BSE images of the various vesuvianite samples were produced in different analytical sessions using different color-scales).

Table 2 ID-TIMS U–Pb analytical results for vesuvianite

Sample[a]	Weight (mg)	Concentrations (μg g^{-1}) U	Pb	^{206}Pb/^{204}Pb Measured ratios[b]	Common lead (μg g^{-1})	Atomic ratios[c] ^{206}Pb/^{238}U	2σ	^{207}Pb/^{235}U	2σ	Rho	^{207}Pb/^{206}Pb	2σ	Apparent ages (Ma)[d] ^{206}Pb/^{238}U	2σ	^{207}Pb/^{235}U	2σ	^{207}Pb/^{206}Pb	2σ
Wilui, Wiluite river, Sakha-Yakutia, Russia																		
Initial Pb[e]: ^{206}Pb/^{204}Pb = 18.2 ± 0.5, ^{207}Pb/^{204}Pb = 15.60 ± 0.15, ^{208}Pb/^{204}Pb = 38.0 ± 0.5																		
V3-1	3.125	11.6	0.5	422.6	0.1	0.0405	0.0004	0.2831	0.0093	0.37	0.0507	0.0015	255.7	2.7	253.1	7.3	229	69
V3-2	1.928	17.3	0.7	586.9	0.1	0.0405	0.0002	0.2845	0.0032	0.38	0.0510	0.0005	255.7	1.0	254.2	2.5	240	24
V3-3	1.210	14.2	0.6	425.9	0.5	0.0404	0.0002	0.2866	0.0054	0.32	0.0514	0.0009	255.4	1.3	255.9	4.3	260	42
V3-4	1.491	14.3	0.6	565.6	0.1	0.0405	0.0002	0.2863	0.0041	0.42	0.0513	0.0007	255.7	1.3	255.6	3.2	255	30
V3-5	1.831	15.2	0.6	638.3	0.1	0.0403	0.0003	0.2831	0.0049	0.49	0.0509	0.0008	254.9	1.9	253.1	3.9	237	35
V3-6	1.092	17.4	0.8	511.4	0.1	0.0404	0.0003	0.2806	0.0066	0.30	0.0504	0.0011	255.3	1.6	251.1	5.2	212	52
V3-7	1.799	15.8	0.7	541.8	0.1	0.0404	0.0003	0.2838	0.0049	0.53	0.0509	0.0008	255.6	2.1	253.7	3.9	236	34
M784, Saima, Liaoning province, China																		
Initial Pb[e]: ^{206}Pb/^{204}Pb = 18.3 ± 0.5, ^{207}Pb/^{204}Pb = 15.60 ± 0.15, ^{208}Pb/^{204}Pb = 38.0 ± 0.5																		
V1-1	0.194	216	17.8	147.3	3.7	0.0354	0.0004	0.2376	0.0084	0.38	0.0487	0.0016	224.1	2.4	216.5	6.8	134	77
V1-2	0.584	211	21.7	146.5	3.7	0.0358	0.0002	0.2476	0.0063	0.17	0.0502	0.0013	226.6	1.3	224.6	5.1	204	58
V1-3	0.265	198	17.6	141.7	3.6	0.0356	0.0003	0.2493	0.0074	0.25	0.0507	0.0015	225.8	1.6	226.0	6.0	228	67
V1-4	0.413	212	20.8	79.6	7.7	0.0353	0.0003	0.2439	0.0126	0.07	0.0501	0.0026	223.9	2.0	221.6	10.4	198	121
V1-5	0.365	232	22.5	79.6	7.9	0.0354	0.0003	0.2454	0.0127	0.09	0.0503	0.0026	224.1	2.0	222.8	10.4	210	121
V1-6	0.485	221	14.6	114.0	4.6	0.0351	0.0002	0.2438	0.0079	0.13	0.0504	0.0016	222.5	1.5	221.5	6.5	211	75
M6635, Saima, Liaoning province, China																		
Initial Pb[e]: ^{206}Pb/^{204}Pb = 17.3 ± 0.5, ^{207}Pb/^{204}Pb = 15.50 ± 0.15, ^{208}Pb/^{204}Pb = 38.0 ± 0.5																		
V2-1	0.476	257	13.9	197.1	3.2	0.0360	0.0002	0.2517	0.0047	0.27	0.0507	0.0009	228.1	1.2	227.9	3.9	226	42
V2-2	0.692	231	13.5	160.7	3.6	0.0360	0.0002	0.2518	0.0058	0.21	0.0507	0.0011	228.3	1.3	228.0	4.7	226	52
V2-3	0.149	222	13.7	143.2	3.9	0.0360	0.0002	0.2478	0.0071	0.16	0.0499	0.0014	228.1	1.2	224.8	5.8	191	66
V2-4	1.051	235	13.2	163.4	3.6	0.0359	0.0003	0.2487	0.0059	0.33	0.0530	0.0011	227.1	1.6	225.5	4.8	209	52
V2-5	0.376	243	13.5	170.3	3.6	0.0360	0.0002	0.2511	0.0053	0.18	0.0505	0.0011	228.2	1.2	227.5	4.3	220	48
V2-6	0.310	238	12.6	183.6	3.2	0.0361	0.0002	0.2516	0.0053	0.24	0.0506	0.0010	228.4	1.2	227.9	4.3	222	48

[a] Small fragments from single vesuvianite crystals. Fragments were selected to show only fresh fracture surfaces. [b] Lead isotope ratios corrected for fractionation, blank, and isotopic tracer. Samples were analyzed at GFZ German Research Centre for Geosciences, Potsdam, Germany, using a ^{205}Pb–^{235}U mixed isotopic tracer. Total blanks were less than 15 pg for lead and less than 1 pg for uranium. [c] Lead corrected for fractionation, blank, isotopic tracer, and initial lead. [d] Apparent ages were calculated using the constants of Jaffey *et al.* (1971) recommended by IUGS: λ^{238} = 1.55125 E-10 y^{-1}, λ^{235} = 9.848 E-10 y^{-1}. [e] Initial lead was estimated using the ^{207}Pb/^{204}Pb *vs.* ^{206}Pb/^{204}Pb diagram. The un-leached samples (V1-4, V1-5, V1-6) have distinctly higher contents of common Pb. Their common Pb as estimated using the ^{207}Pb/^{204}Pb *vs.* ^{206}Pb/^{204}Pb diagram is less radiogenic (^{206}Pb/^{204}Pb = 16.3 ± 0.5, ^{207}Pb/^{204}Pb = 15.50 ± 0.15, ^{208}Pb/^{204}Pb = 38.0 ± 0.5) than the common Pb used for the leached samples.

Table 3 Compilation of U–Pb LA-SF-ICP-MS dating results of vesuvianite

		Pb (μg g^{-1})	Th (μg g^{-1})	U (μg g^{-1})	Th/U	f_{206} [a] (%)		Intercept age ^{206}Pb/^{238}U (Ma)		
Sample	n	(2SD)	(2SD)	(2SD)	(2SD)	Mean	2SD	Mean	2SD	ID-TIMS age[b] (Ma) (2SD)
Wilui	18	0.30 (0.25)	1.70 (7.42)	10.3 (9.4)	0.20 (0.98)	1.9	1.7	255.5	2.8	255.5 (0.6)
M784	21	10.9 (6.7)	153 (281)	102 (115)	2.00 (5.01)	22.6	22.8	223.8	3.5	224.8 (1.8)
M6635	21	14.9 (4.0)	213 (129)	190 (63)	1.15 (0.88)	10.3	5.5	230.8	2.7	228.1 (0.5)
	112	13.7 (5.2)	193 (159)	239 (78)	0.84 (0.81)	8.9	3.7	229.8	1.3	
M1377	21	6.79 (2.02)	55.9 (36.0)	76.9 (31.3)	0.74 (0.41)	17.0	10.8	225.0	3.3	
Bufa	30	1.90 (1.11)	13.7 (10.2)	245 (73)	0.06 (0.04)	4.4	8.2	30.8	0.3	31.6 (0.3)
M659	21	5.92 (8.32)	148 (596)	109 (133)	0.82 (3.06)	12.0	11.6	155.4	2.0	
M660	21	5.31 (3.09)	23.8 (47.1)	104 (91)	0.21 (0.33)	15.4	13.5	156.5	2.7	
M1439	19	3.10 (2.24)	5.2 (16.1)	37.6 (56.8)	0.15 (0.38)	30.6	24.0	158.5	3.1	
M6599	21	0.50 (0.58)	0.80 (2.49)	3.05 (6.15)	0.25 (0.61)	58.9	43.9	157.3	4.6	
M6601	21	0.42 (0.61)	4.95 (13.37)	5.06 (8.55)	1.21 (2.39)	43.0	33.5	93.3	2.5	
M6608	17	1.35 (2.37)	1.48 (4.62)	61.6 (134.4)	0.025 (0.087)	15.4	32.0	88.4	1.4	

[a] f_{206}, common ^{206}Pb in total ^{206}Pb; f_{206} = [(^{207}Pb/^{206}Pb)total – (^{207}Pb/^{206}Pb)radiogenic]/[(^{207}Pb/^{206}Pb)init – (^{207}Pb/^{206}Pb)radiogenic]. [b] ID-TIMS age: Concordia age of Bufa from Romer and Heinrich, 1998, other ID-TIMS ages from this study.

Ma to 255.7 ± 1.0 Ma. The seven aliquots yield a concordant ^{206}Pb/^{238}U age of 255.5 ± 0.6 Ma (2σ, MSWD = 3.8) (Fig. 3a).

Vesuvianite samples M784 and M6635 were collected from the Saima complex located on the Liaodong Peninsula of northern China. Six fractions of sample M784 were analyzed. To test whether washing with warm 1 mol L^{-1} HNO_3 removes common Pb, *i.e.*, results in higher measured ^{206}Pb/^{204}Pb, three fractions were washed with HNO_3 and three fractions were not washed. The acid-treated samples (V1-1, V1-2 and V1-3) gave measured ^{206}Pb/^{204}Pb ratios in the range from 141.7 to 147.3, whereas the non-acid-washed samples (V1-4, V1-5 and V1-6) gave lower ^{206}Pb/^{204}Pb ratios in the range from 79.6 to 114.0. The common Pb contents of the acid-treated and untreated samples fall in the ranges from 3.6 to 3.7 μg g^{-1}and from 4.6 to 7.9 μg g^{-1}, respectively. The uranium contents range from 198 to 232 μg g^{-1} and there is no systematic difference in U content between acid-treated and untreated samples. The initial Pb isotope composition of acid-treated and untreated samples, estimated using the ^{206}Pb/^{204}Pb *vs.* ^{238}U/^{204}Pb and ^{207}Pb/^{204}Pb *vs.* ^{206}Pb/^{204}Pb diagram, are different: The acid-treated samples give a more radiogenic initial Pb isotopic composition (^{206}Pb/^{204}Pb = 18.3 ± 0.5, ^{207}Pb/^{204}Pb = 15.60 ± 0.15, ^{208}Pb/^{204}Pb = 38.0 ± 0.5) than the untreated samples (^{206}Pb/^{204}Pb = 16.3 ± 0.5, ^{207}Pb/^{204}Pb = 15.50 ± 0.15, ^{208}Pb/^{204}Pb = 38.0 ± 0.5). As the untreated samples have important contributions of common Pb, we used the less radiogenic initial Pb isotopic composition for the common Pb correction. Using different initial Pb isotopic compositions for acid-treated and untreated samples yields ^{206}Pb/^{238}U and ^{207}Pb/^{235}U data that overlap within analytical error in the concordia diagram (grey circles; Fig. 3b). The apparent ^{206}Pb/^{238}U age ranges from 222.5 ± 1.5 Ma to 226.6 ± 1.3 Ma. Together, the six analyses define a concordant ^{206}Pb/^{238}U age of 224.7 ± 0.7 Ma (2σ, MSWD = 3.0). For comparison, the three acid-treated samples yield a concordant ^{206}Pb/^{238}U age of 226.0 ± 2.6 Ma (2σ, MSWD = 1.7). These results agree well with our laser ablation results and earlier reported age data (230–224 Ma, Zhu *et al.*[29]). The initial Pb isotopic composition and the distinctively higher common Pb of the untreated samples indicate that the easily dissolved component (*e.g.*, carbonates) has a different initial Pb isotopic composition and washing with dilute HNO_3 is a helpful step to obtain higher bulk-^{206}Pb/^{204}Pb values for ID-TIMS U–Pb dating.

Six fractions of M6635 vesuvianite were analyzed. The isotopic compositions of the individual fractions fall in the ^{206}Pb/^{204}Pb range of 143.2 and 197.1 (Table 2). Common Pb ranges from 3.2 to 3.9 μg g^{-1} and U ranges from 222 to 257 μg g^{-1}, respectively. In a ^{206}Pb/^{238}U *vs.* ^{207}Pb/^{235}U diagram, all M6635 vesuvianite analyses are concordant and overlap with each other. The apparent ^{206}Pb/^{238}U age ranges from 227.1 ± 1.6 Ma to 228.4 ± 1.2 Ma. Six aliquots constrain a concordant ^{206}Pb/^{238}U age of 228.1 ± 0.6 Ma (2σ, MSWD = 0.9) (Fig. 3c). The ID-TIMS U–Pb age agrees well with our results of laser ablation dating and the previously reported age data (230–224 Ma, Zhu *et al.*[29]).

3.2 Protocol validation for laser ablation analyses

Wiluite vesuvianite is an approximately 1 × 1.5 × 2 cm specimen of rodingitized Mg–Ca-skarn. Wiluite crystals occur in a hydrogarnet-chlorite-serpentinite matrix together with small crystals of fassaitic pyroxene and Ti-bearing andradite-grossular. The skarn formed at the contact of the Siberian trap with Ordovician carbonate rocks. This relatively uncommon specimen contains isolated dark green, tetragonal vesuvianite crystals with well-developed prism faces and double termination. The dated sample is a B rich vesuvianite and has an average U content of 10.3 ± 9.4 μg g^{-1} (2σ, n = 18). The measured f_{206} ranges from 1.1 to 3.7%. All eighteen analyses cluster close to the concordia, yielding an intercept age of 255.5

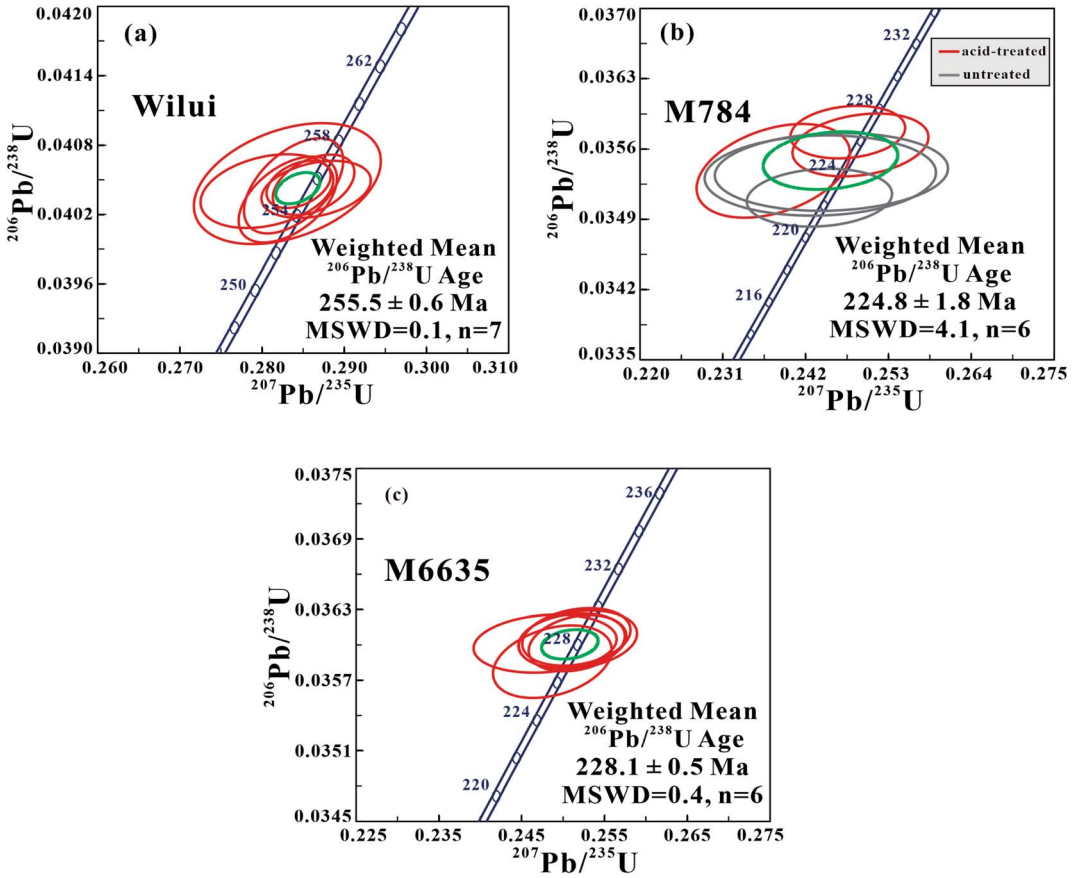

Fig. 3 Concordia diagrams for ID-TIMS data of vesuvianite samples (a) Wilui (Russia), (b) M784 (Saima), and (c) M6635 (Saima). The concordia age of each sample is shown as the green ellipse. The weighted concordia age of both acid-treated (red lines) and untreated (gray lines) vesuvianite samples M784. Diagrams and ages calculated using Isoplot (Ludwig, 2003).[20] Error ellipses represent 2σ uncertainties.

$\pm$ 2.8 Ma (2σ, n = 18) in the Tera–Wasserburg diagram, which is consistent with the ^{207}Pb-corrected weighted mean ^{206}Pb/^{238}U age of 255.5 $\pm$ 2.8 Ma (2σ) (Fig. 4a). The upper intercept was anchored using a ^{207}Pb/^{206}Pb value of 0.8525 according to the terrestrial Pb evolution model of Stacey and Kramers.[27] This result agrees well with the here presented ID-TIMS age of 255.5 $\pm$ 0.6 Ma (2σ, n = 7). This is the first U–Pb age of vesuvianite from the Vilyui River, Yakutia, Russia.[30] Note, for vesuvianite samples with low common Pb contents as Wilui, a fixed ^{207}Pb/^{206}Pb value (measured on cogenetic phases or estimated from the S–K model) should be used to anchor the intercept age in the Tera–Wasserburg diagram, as unconstrained data overestimate the uncertainties. For instance, unanchored regression yields for the above data a concordia intercept of 257.7 $\pm$ 7.3 Ma (MSWD = 0.03) in the Tera–Wasserburg diagram and a meaningless ^{207}Pb/^{206}Pb intercept of 1.6 $\pm$ 4.1 (Fig. 4a).

Vesuvianite samples M784, M6635, and M1377 were collected from the Saima complex located on the Liaodong Peninsula of northern China. Vesuvianite sample M784 is an about 5 × 8 × 6 cm large specimen. Vesuvianite crystals have U concentrations ranging from 56 to 230 μg g^{-1}. f_{206} values of the laser ablation spot analyses range from 6% to 44%. The intercept age of vesuvianite M784 in the Tera–Wasserburg diagram is 223.8 $\pm$ 3.5 (2σ, n = 21, MSWD = 0.16), which is consistent with the ^{207}Pb-corrected weighted mean ^{206}Pb/^{238}U age of 224.1 $\pm$ 2.9 Ma (2σ) (Fig. 4b). This result is identical to the ID-TIMS U–Pb vesuvianite age of 224.8 $\pm$ 1.8 Ma (2σ, n = 6) obtained in this work. The un-anchored discordia intercepts in the Tera–Wasserburg diagram at a ^{207}Pb/^{206}Pb value of 0.827 $\pm$ 0.042 and yields an age of 222.7 $\pm$ 4.4 Ma (MSWD = 0.15). For comparison, the Stacey and Kramers Pb model yields a ^{207}Pb/^{206}Pb of 0.8503.[27] Vesuvianite sample M6635 is an about 8 × 11 × 4 cm large specimen. Vesuvianite crystals have U concentrations ranging from 104 to 313 μg g^{-1}. The sample has the highest U content among the studied samples. f_{206} of laser ablation spot analyses ranges from 7% to 14%. The intercept age of vesuvianite sample M6635 in the Tera–Wasserburg diagram is 230.8 $\pm$ 2.7 (2σ, n = 21, MSWD = 0.12), which is consistent with the ^{207}Pb-corrected weighted mean ^{206}Pb/^{238}U age of 230.8 $\pm$ 2.5 Ma (2σ; Fig. 4c). This result is consistent with the here presented ID-TIMS U–Pb vesuvianite age of 228.1 $\pm$ 0.5 Ma (2σ, n = 6). Vesuvianite sample M6635 was analyzed in several analytical sessions. 112 analyses from seven sessions yield an intercept age of 229.8 $\pm$ 1.3 (2σ, n = 112, MSWD = 0.11) in the Tera–Wasserburg diagram, which is consistent with the ^{207}Pb corrected weighted mean ^{206}Pb/^{238}U age of 229.9 $\pm$ 0.9 Ma (2σ; Fig. 4d). These analytical data show that the analytical protocol produces reproducible results. The unconstrained discordia in

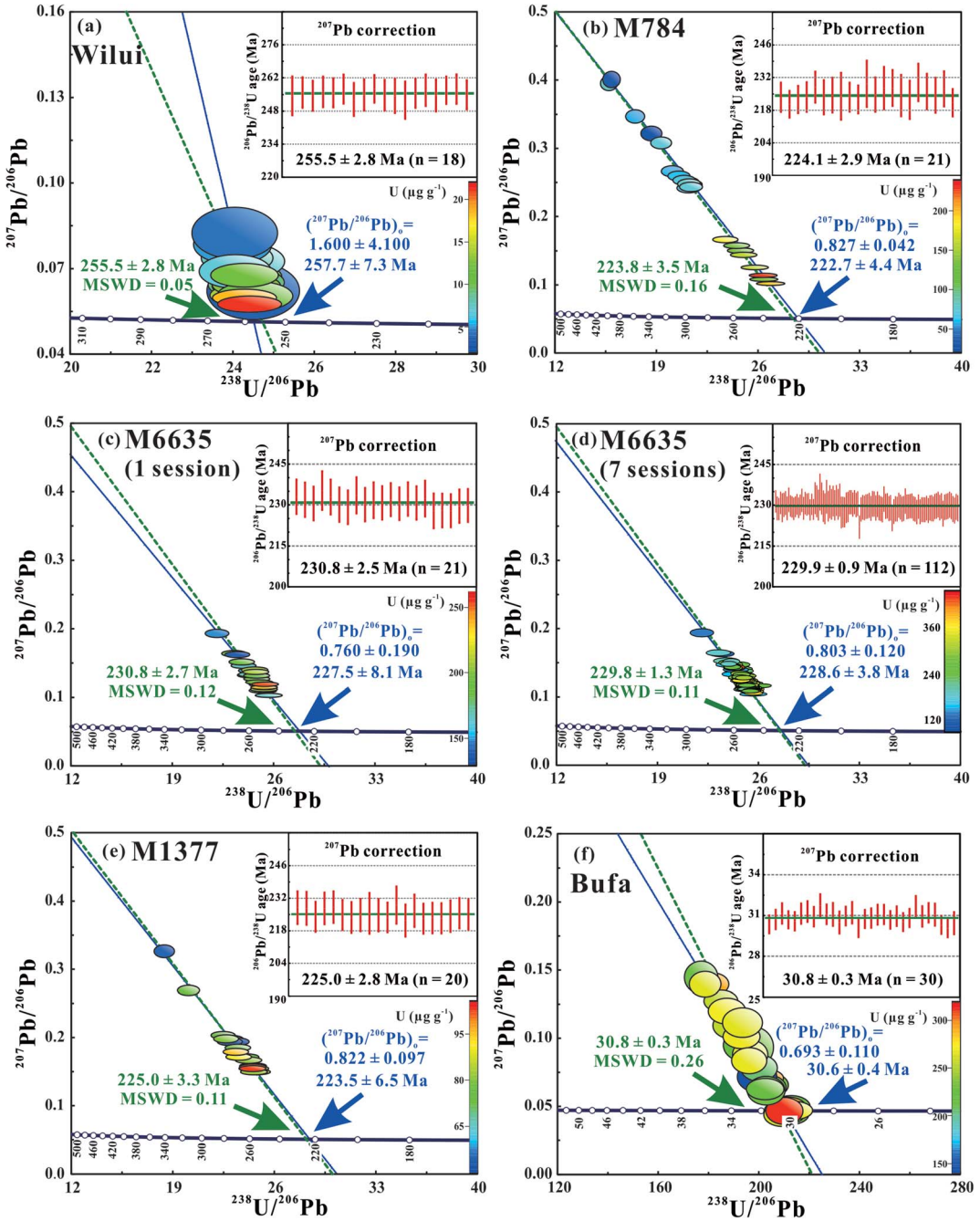

Fig. 4 Terra–Wasserburg diagrams for LA-SF-ICP-MS data of vesuvianite samples (a) Wilui, (b) M784, (c and d) M6635, (e) M1377, and (f) Bufa. The green dotted discordia lines in the Terra–Wasserburg diagrams are forced through a ^{207}Pb/^{206}Pb value of 0.82 ± 0.02 for vesuvianite Bufa and 0.85 ± 0.02 for all other vesuvianite samples. The ^{207}Pb/^{206}Pb values were estimated using the initial Pb isotope composition of sample Bufa or two-stage crustal Pb model of Stacey and Kramers (1975) for others.[4,27] Data were plotted and evaluated using Isoplot (Ludwig, 2003).[20] The unconstrained discordias are shown as blue solid lines. Error bars in the insets are at the 1σ level.

the Tera–Wasserburg diagram yields a ^{207}Pb/^{206}Pb ratio of 0.803 ± 0.120 ($S\&K$ = 0.8506 (ref. 27)) and an intercept age of 228.6 ± 3.8 Ma (MSWD = 0.08).

Vesuvianite sample M1377 has U contents ranging from 52 to 85 μg g^{-1} and variable f_{206} values of 12% to 34%. Twenty analyses yield an intercept age of 225.0 ± 3.3 Ma (2σ, MSWD = 0.11; Fig. 4e), which is consistent with the ^{207}Pb-corrected weighted mean ^{206}Pb/^{238}U age of 225.0 ± 2.8 Ma (2σ, n = 20). The upper intercept was anchored using a ^{207}Pb/^{206}Pb value of 0.8508 derived from the Stacey and Kramers terrestrial Pb evolution model.[27] The unconstrained discordant intercepts at a ^{207}Pb/^{206}Pb value of 0.822 ± 0.097 and yields an age of 223.5 ± 6.5 Ma (MSWD = 0.11) in the Tera–Wasserburg diagram.

The three vesuvianite samples investigated yield ages that overlap within analytical uncertainties. The *in situ* and ID-TIMS U–Pb ages of the three vesuvianite samples agree well with

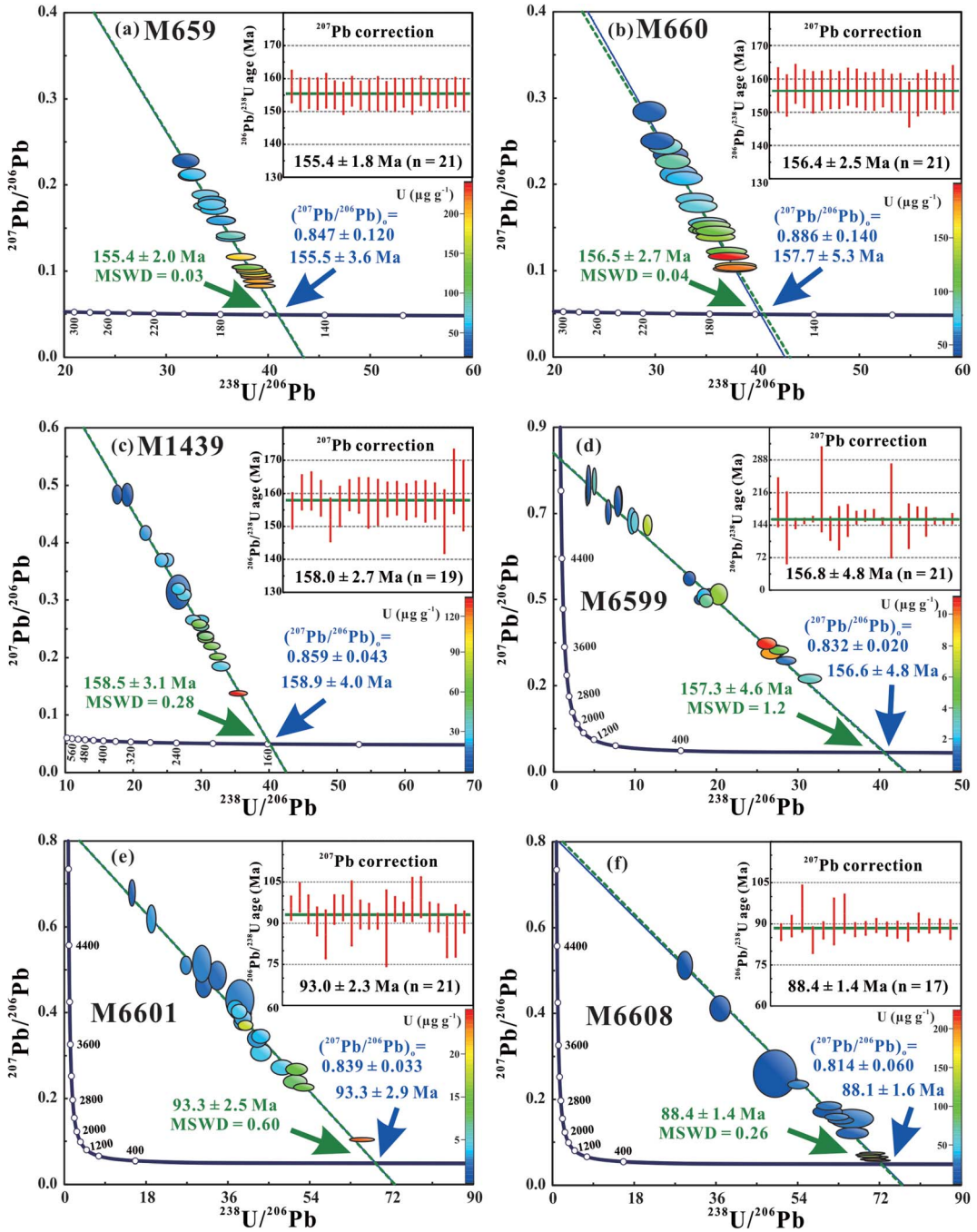

Fig. 5 Terra–Wasserburg diagrams for LA-SF-ICP-MS data of vesuvianite samples (a) M659, (b) M660, (c) M1439, (d) M6599, (e) M6601, and (f) M6608. The green dotted discordia lines in the Terra–Wasserburg diagrams are forced through a ^{207}Pb/^{206}Pb value of 0.84 ± 0.02 for vesuvianite samples M6601 and M6608 and 0.85 ± 0.02 for all other vesuvianite samples. The ^{207}Pb/^{206}Pb values were estimated using the two-stage crustal Pb model of Stacey and Kramers (1975).[27] The unconstrained discordias are shown as blue solid lines. Error bars in the insets are at the 1σ level. Data were plotted and evaluated using Isoplot (Ludwig, 2003).[20]

earlier reported LA-ICP-MS and SIMS U–Pb zircon ages of 230–224 Ma (ref. 29) and are interpreted to represent the crystallization ages of the nepheline syenites, quartz-bearing syenites, and volcanic rocks.

The vesuvianite sample Bufa from a Tertiary alkaline igneous complex in the Sierra de San Carlos (northeastern Mexico) has a relatively broad range of f_{206} values from 0.1% to ~13%. All LA-SF-ICP-MS data plotted on the Tera–Wasserburg diagram produce an intercept age of 30.8 ± 0.3 Ma (2σ, $n = 30$, MSWD = 0.26), which is identical to the ^{207}Pb-corrected weighted mean ^{206}Pb/^{238}U age of 30.8 ± 0.3 Ma (2σ, $n = 30$; Fig. 4f). The upper intercept was anchored using a ^{207}Pb/^{206}Pb value of 0.8232 derived from the initial Pb isotope composition of sample Bufa measured by ID-TIMS.[4] The unconstrained discordant

intercepts at a $^{207}Pb/^{206}Pb$ value of 0.693 ± 0.110 and yields an age of 30.6 ± 0.4 Ma (MSWD = 0.27) in the Tera–Wasserburg diagram. For comparison, the Stacey and Kramers model has $^{207}Pb/^{206}Pb$ = 0.8376 for 31 Ma common Pb.[27] The $^{207}Pb/^{206}Pb$ intercept of 0.693 indicates that the common Pb of vesuvianite in part is derived from the carbonates, which in organic-rich sections may have more radiogenic Pb isotopic compositions. Furthermore, the relative contribution of Pb from the carbonates and the magmatic fluid may differ during vesuvianite growth or among different vesuvianite crystals, possibly explaining the slightly older $^{206}Pb/^{238}U$ ID-TMS age (31.6 ± 0.3 Ma; 2σ, n = 3) of another crystal from the same outcrop.[4]

3.3 Practical application

Vesuvianite samples M659, M660, and M1439 from the Dengjiaxian ore deposit, Chenzhou, Hunan province, China, are expected to yield U–Pb ages similar to the ~160–155 Ma mineralization age range known from W–Sn ore deposits in the Nanling region, southern China.[14,17,31,32] Vesuvianite samples M659 and M660 have U contents in the range from 52 to 221 μg g^{-1} and a relatively narrow f_{206} range from 4% to ~30%. In the Tera–Wasserburg diagram, vesuvianite samples M659 and M660 yield intercept ages of 155.4 ± 2.0 Ma (2σ, n = 21) and 156.5 ± 2.7 Ma (2σ, n = 21), respectively, consistent with the ^{207}Pb-corrected weighted mean $^{206}Pb/^{238}U$ age of 155.4 ± 1.8 Ma (2σ, n = 21) and 156.4 ± 2.5 Ma (2σ, n = 21), respectively (Fig. 5a and b). The unconstrained discordias for vesuvianite samples M659 and M660 yield $^{207}Pb/^{206}Pb$ intercepts of 0.847 ± 0.120 and 0.886 ± 0.140, respectively, which are similar to that of 155–156 Ma common Pb of the Stacey and Kramers Pb model,[27] and intercept ages of 155.5 ± 3.6 Ma (MSWD = 0.04) and 157.7 ± 5.3 Ma (MSWD = 0.03), respectively, in the Tera–Wasserburg diagram. Vesuvianite sample M1439 has (generally lower) U contents in the range from 6.1 to 129 μg g^{-1} and a broader f_{206} range of 11% to 55%. In the Tera–Wasserburg diagram, these data yield an intercept age of 158.5 ± 3.1 Ma (2σ, n = 19), consistent with the ^{207}Pb-corrected weighted mean $^{206}Pb/^{238}U$ age of 158.0 ± 2.7 Ma (2σ, n = 19; Fig. 5c). The unconstrained discordia yields a $^{207}Pb/^{206}Pb$ intercept of 0.859 ± 0.043, which is similar to that of model Pb for that age (0.8459 (ref. 27)), and an intercept age of 158.9 ± 4.0 Ma (MSWD = 0.29) in the Tera–Wasserburg diagram .

It is not known from which deposit in the Guangxi province the vesuvianite samples M6599, M6601, and M6608 are derived. Generally, these vesuvianite samples have highly variable U and common Pb contents (Fig. 5d–f). Vesuvianite sample M6599 has U contents in the range from 0.3 to 10.7 μg g^{-1}, f_{206} in the range from 24% to 89%, and yields an intercept age of 157.3 ± 4.6 Ma (2σ, n = 21) in the Tera–Wasserburg diagram. In the Tera–Wasserburg diagram, the unconstrained discordia has a $^{207}Pb/^{206}Pb$ intercept of 0.832 ± 0.020 (model common Pb for 157 Ma has a $^{207}Pb/^{206}Pb$ ratio of 0.8458 (ref. 27)) and an intercept age of 156.6 ± 4.8 Ma (MSWD = 1.30) (Fig. 5d). In contrast, vesuvianite samples M6601 and M6608 have U contents ranging from 1.5 to 188 μg g^{-1}, have f_{206} ranging from 2% to 72%, and yield intercept ages of 93.3 ± 2.5 Ma (2σ, n = 21) and 88.4 ± 1.4 Ma (2σ, n = 17), respectively, in the Tera–Wasserburg diagram. These ages are consistent with the ^{207}Pb-corrected weighted mean $^{206}Pb/^{238}U$ ages of 93.0 ± 2.3 Ma (2σ, n = 21) and 88.4 ± 1.4 Ma (2σ, n = 21), respectively (Fig. 5e and f). The unconstrained discordias for vesuvianite samples M6601 and M6608 yield $^{207}Pb/^{206}Pb$ intercepts of 0.839 ± 0.033, and 0.814 ± 0.060, respectively, which is similar to that of common Pb of the Stacey and Kramers Pb model for that age,[27] and intercept ages of 93.3 ± 2.9 Ma (MSWD = 0.63) and 88.1 ± 1.6 Ma (MSWD = 0.25), respectively, in the Tera–Wasserburg diagram. These vesuvianite ages all fall in the age range known for Sn–W deposits of South China (*e.g.*, Mao *et al.*[32]).

3.4 Closure temperature

Vesuvianite is stable over a broad range of temperatures (300–980 °C), fluid and rock compositions, and f_{O2} values.[33] Vesuvianite is susceptible to alteration during later stages of hydrothermal activity. Such alteration could disturb or reset the original U–Pb isotopic system, but is readily revealed by petrographic observations. The U–Pb system may potentially also be disturbed by Pb loss, which would result in too young ages. To estimate whether unaltered vesuvianite dates crystallization or a later time, we calculated the temperature of closure for Pb of vesuvianite using the method of Zhao and Zheng[33] for a nominal grain size of 100 μm and cooling rates of 10–200 °C Ma^{-1} (Fig. 6). The calculated closure temperatures for Pb fall in the range of 650–900 °C (Fig. 6). These values are higher than the temperatures of 300–600 °C typically encountered in contact metamorphic limestones[4] and skarn mineralization[34] in the upper crust. Hence, the age of unaltered vesuvianite dates the time of vesuvianite formation rather than later isotopic closure. Thus, unaltered vesuvianite may be a reliable U–Pb chronometer for mineral deposits, especially those that do not have other datable minerals.

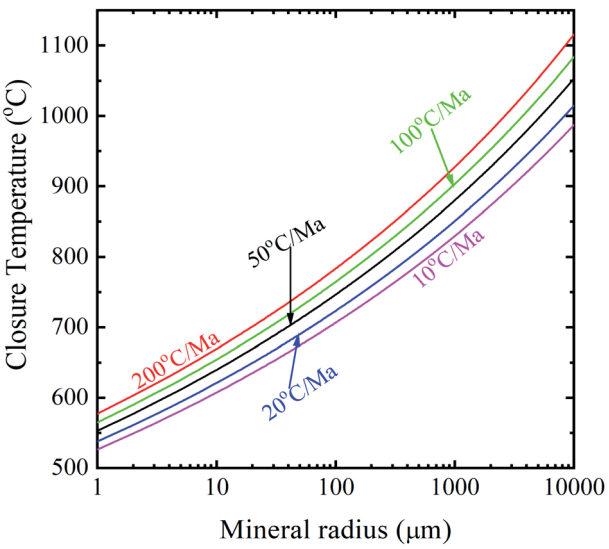

Fig. 6 Calculation of Pb closure temperatures for vesuvianite based on the method of Zhao and Zheng (2007).[33]

3.5 Matrix effects for schorlomite and vesuvianite

Schorlomite and vesuvianite have similar contents of CaO (32–34 wt%) and SiO_2 (34–36 wt%). However, there is some difference in the content of Al_2O_3 between schorlomite and vesuvianite, where the former contains 1–3 wt% Al_2O_3 and the latter contains 12–17 wt% Al_2O_3. To further evaluate the influence of matrix effects, we employed vesuvianite Wilui, which is characterized by the lowest common Pb contents (0.1 to 0.5 μg g^{-1}) among the analyzed samples, as the external calibration standard to calculate other vesuvianite crystals. As shown in Fig. 7a, intercept age obtained for vesuvianite sample M784 in the Tera–Wasserburg diagram using Wilui as the external calibration standard is 224.0 ± 2.2 (2σ, n = 23, MSWD = 0.02), which agrees well with the intercept age using the schorlomite PL34 as the primary reference material. Similarly, the intercept age for vesuvianite M6635 in the Tera–Wasserburg diagram is 228.3 ± 1.9 (2σ, n = 23, MSWD = 0.03, Fig. 7b), which is identical to the schorlomite PL34 corrected intercept age of 230.8 ± 2.7 (2σ, n = 21, MSWD = 0.12) obtained in this work. The vesuvianite sample Bufa is employed to use as a secondary reference material for quality control. Twenty-four analyses of sample Bufa using vesuvianite Wilui as the external calibration standard yielded a U–Pb Tera–Wasserburg concordia intercept age of 31.4 ± 0.7 Ma (Fig. 7c) with an MSWD = 0.34, which is identical to the schorlomite PL34 corrected intercept age of 30.8 ± 0.3 (2σ, n = 30, MSWD = 0.26). The unconstrained discordia in the Tera–Wasserburg diagram yields a $^{207}Pb/^{206}Pb$ intercept of 0.772 ± 0.026, similar to the upper intercept value of 0.693 ± 0.110 obtained by using the schorlomite PL34 as the primary reference material. These data demonstrate clearly that the matrix effects between schorlomite and vesuvianite during laser ablation are insignificant and the used analytical protocol is robust.

3.6 Reference material

The ideal U–Pb reference material is characterized by relatively high contents of U and low contents of common Pb, as well as a low variance of the U–Pb ratios. Among the eleven vesuvianite samples investigated here, there are four samples that seem to be particularly suited as a primary or secondary reference material, *i.e.*, vesuvianite samples M6635, Wilui, M784, and Bufa. Vesuvianite sample M6635 has the highest U contents among the analyzed samples, has relatively low contributions of common Pb and produces consistent analytical results both within a single session and between different sessions (Fig. 4c and d and 8, Table 3). It is recommended as a primary reference material. Vesuvianite Wilui is characterized by the lowest common Pb contents among the analyzed samples, but has distinctly lower U contents than vesuvianite sample M6635 (Fig. 8, Table 3). This vesuvianite is a suitable primary reference material, in particular when instrument sensitivity improves in the future. Note, there are vesuvianite samples with U contents in the range of several thousand μg g^{-1} to several wt%.[1] Such samples are not suited as reference materials because of the following reason. The α-decay of ^{238}U, ^{235}U and ^{232}Th (and some daughter nuclei of their respective decay series) induced major

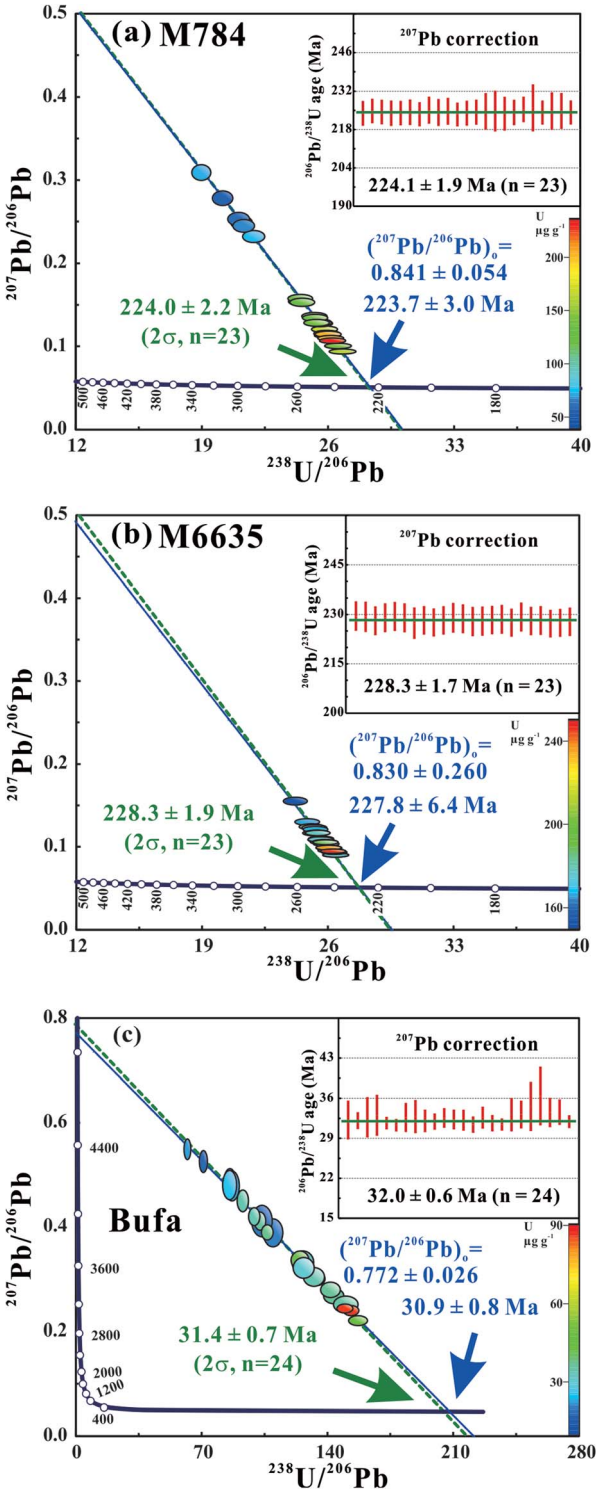

Fig. 7 Terra–Wasserburg diagrams for LA-SF-ICP-MS data of vesuvianite samples (a) M784, (b) M6635, and (c) Bufa. The green dotted discordia lines in the Terra–Wasserburg diagrams are forced through a $^{207}Pb/^{206}Pb$ value of 0.82 ± 0.02 for vesuvianite Bufa, measured by ID-TIMS,[4] and 0.85 ± 0.02 for the other two vesuvianite samples, estimated using the two-stage crustal Pb model of Stacey and Kramers (1975).[4,27] The blue solid lines are unconstrained discordia lines. Vesuvianite Wilui was used as a primary reference material to calculate other vesuvianite samples (M784, M6635, and Bufa). Data were plotted and evaluated using Isoplot (Ludwig, 2003).[20] Error bars in the insets are at the 1σ level.

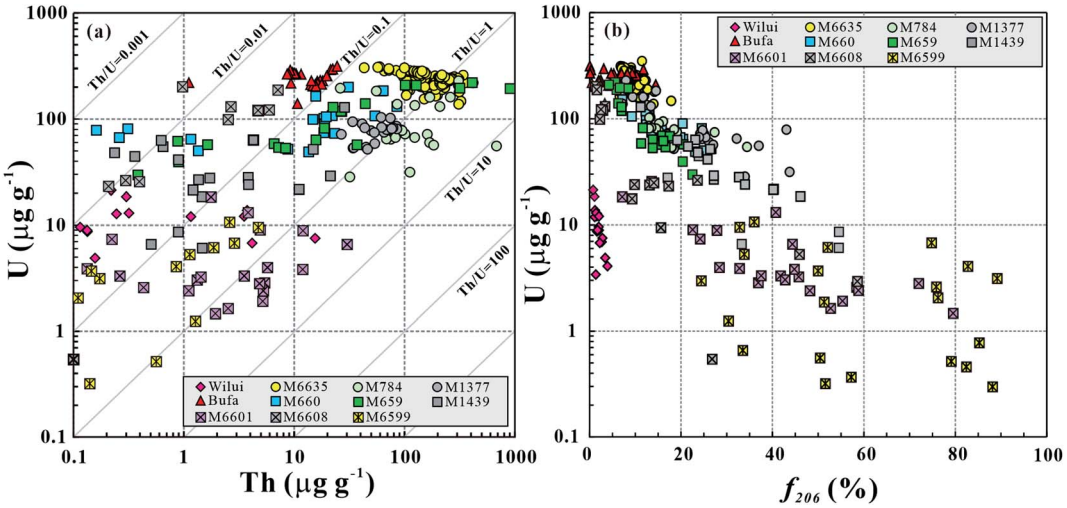

Fig. 8 (a) Th and U concentrations and corresponding Th/U ratios typically are variable within individual vesuvianite samples. (b) The contents of U and the portion of common Pb are broadly correlated as most samples have a Mesozoic age and illustrate that samples with low U contents are unlikely to produce precise ages. There are two vesuvianite samples deviating from this general pattern, *i.e.*, Wilui and Bufa, that are both characterized by unusually low contents of common Pb. These samples have developed low f_{206} despite moderate U content (Wilui) or young age (Bufa).

lattice damage by emission of an α-particle and by α-recoil of the daughter nucleus. The cumulative damage eventually results in open system behavior of the U–Pb system (*e.g.*, Romer[35]).

Vesuvianite sample M784, which has relatively high and homogenous U contents, is not suited as the primary reference material because of its variable and in part relatively high contents of common Pb, which is obvious from the broad range of measured $^{207}Pb/^{206}Pb$ values. This sample, however, is highly suited as a secondary reference material for *in situ* analysis. Vesuvianite sample Bufa has variable U contents and variable contributions of common Pb, which results in a relatively broad range of $^{207}Pb/^{206}Pb$ values (Fig. 4f). Because of this heterogeneity, as well as its young age, vesuvianite sample Bufa is not suited to be a primary reference material, but represents a useful secondary reference material for quality control.

4. Conclusions

Vesuvianite is a common mineral in skarn ore deposits, as well as in metamorphic and metasomatic argillaceous carbonate rocks. U–Pb dating of vesuvianite growth directly dates the formation of skarn mineralization or the metamorphism or metasomatism of argillaceous limestones. We established an analytical protocol for *in situ* U–Pb age dating of vesuvianite by LA-SF-ICP-MS. We used Ti-bearing andradite (schorlomite), which has a similar major element composition to vesuvianite, as the reference material for U–Pb dating of vesuvianite by LA-SF-ICP-MS. We tested the robustness of the analytical protocol by U–Pb dating of four vesuvianite samples using ID-TIMS. The close correspondence of ages determined by ID-TIMS and LA-SF-ICP-MS demonstrates the feasibility of our analytical protocol. The high sensitivity, speed, and relatively low cost of LA-SF-ICP-MS dating of vesuvianite series minerals, in combination with a high spatial resolution, may make vesuvianite the mineral of choice for the dating of skarn-type mineralization in the future.

Conflicts of interest

There are no conflicts to declare.

Acknowledgements

This study was financially supported by the Natural Science Foundation of China (No 42173034 & 41688103). The work of Ming Yang at GFZ was supported by a CSC student scholarship (202004910582). We are indebted to Xiang-Zhao Yang and Tony Nikischer for providing vesuvianite samples.

References

1 G. R. Himmelberg and T. P. Miller, *Am. Mineral.*, 1980, **65**, 1020–1025.
2 L. A. Groat, F. C. Hawthorne and T. S. Ercit, *Can. Mineral.*, 1992, **30**, 19–48.
3 R. L. Romer, *Mineral. Petrol.*, 1992, **46**, 331–341.
4 R. L. Romer and W. Heinrich, *Contrib. Mineral. Petrol.*, 1998, **131**, 155–177.
5 M. Fukuyama, M. Ogasawara, H. Sato, D. Ishiyama and T. Nishiyama, *Can. Mineral.*, 2012, **50**, 1373–1386.
6 S. Guo, Y. Chen, C. Z. Liu, J. G. Wang, B. Su, Y. J. Gao, F. Y. Wu, S. Kyaing, Y. H. Yang and Q. Mao, *J. Asian Earth Sci.*, 2016, **117**, 82–106.
7 H. Su, X. J. Wang, Z. M. Chen and S. Z. Li, *Acta Mineral. Sin.*, 2016, **36**, 529–534, (in Chinese with English abstract).
8 J. Xu, C. L. Ciobanu, N. J. Cook, Y. Zheng, X. Sun and B. P. Wade, *Lithos*, 2016, **262**, 213–231.

9 T. L. Panikorovskii, N. V. Chukanov, V. S. Rusakov, V. V. Shilovskikh, A. S. Mazur, G. Balassone, G. Y. Ivanyuk and S. V. Krivovichev, *Minerals*, 2017, **7**, 248.
10 N. V. Chukanov, T. L. Panikorovskii, A. G. Goncharov, I. V. Pekov, D. I. Belakovskiy, S. N. Britvin, S. Möckel and S. A. Vozchikova, *Eur. J. Mineral.*, 2019, **31**, 637–646.
11 F. P. Caucia, L. Marinoni, M. Scacchetti, M. P. Riccardi and O. Bartoli, *Minerals*, 2020, **10**, 535.
12 S. Seman, D. F. Stockli and N. M. McLean, *Chem. Geol.*, 2017, **460**, 106–116.
13 S. T. Wu, M. Yang, Y. H. Yang, L. W. Xie, C. Huang, H. Wang and J. H. Yang, *Int. J. Mass Spectrom.*, 2020, **456**, 116394.
14 Y. H. Yang, M. Yang, H. Wang, J. H. Yang and F. Y. Wu, *Sci. China Earth Sci.*, 2021, **64**, 187–190.
15 P. J. Sylvester and S. E. Jackson, *Elements*, 2016, **12**, 307–310.
16 Y. H. Yang, F. Y. Wu, Q. L. Li, Y. Rojas-Agramonte, J. H. Yang, Y. Li, Q. Ma, L. W. Xie, C. Huang, H. R. Fan, Z. F. Zhao and C. Xu, *Geostand. Geoanal. Res.*, 2019, **43**, 543–565.
17 M. Yang, Y. H. Yang, S. T. Wu, R. L. Romer, X. D. Che, Z. F. Zhao, W. S. Li, J. H. Yang, F. Y. Wu, L. W. Xie, C. Huang, D. Zhang and Y. Zhang, *J. Anal. At. Spectrom.*, 2020, **35**, 2191–2203.
18 Q. Ma, N. J. Evans, X. X. Ling, J. H. Yang, F. Y. Wu, Z. D. Zhao and Y. H. Yang, *Geostand. Geoanal. Res.*, 2019, **43**, 355–384.
19 R. Schmid, R. L. Romer, L. Franz, R. Oberhänsli and G. Martinotti, *J. Metamorph. Geol.*, 2003, **21**, 531–538.
20 K. R. Ludwig, *Isoplot 3.23*, 2003, vol. 3, pp. 1–70.
21 F. Y. Wu, R. H. Mitchell, Q. L. Li, C. Zhang and Y. H. Yang, *Geol. Mag.*, 2017, **155**, 217–236.
22 Y. H. Yang, F. Y. Wu, J. H. Yang, R. H. Mitchell, Z. F. Zhao, L. W. Xie, C. Huang, Q. Ma, M. Yang and H. Zhao, *J. Anal. At. Spectrom.*, 2018, **33**, 231–239.
23 S. T. Wu, G. Wörner, K. P. Jochum, B. Stoll, K. Simon and A. Kronz, *Geostand. Geoanal. Res.*, 2019, **43**, 567–584.
24 C. Paton, J. Hellstrom, B. Paul, J. Woodhead and J. Hergt, *J. Anal. At. Spectrom.*, 2011, **26**, 2508–2518.
25 W. L. Griffin, W. J. Powell, N. J. Pearson and S. Y. O'Reilly, *Mineral. Assoc. Can., Short Course Handb.*, 2008, **40**, 308–311.
26 D. M. Chew, J. A. Petrus and B. S. Kamber, *Chem. Geol.*, 2014, **363**, 185–199.
27 J. S. Stacey and J. D. Kramers, *Earth Planet. Sci. Lett.*, 1975, **26**, 207–221.
28 M. S. A. Horstwood, J. Kosler, G. Gehrels, S. E. Jackson, N. M. McLean, C. Paton, N. Peason, K. Sircombe, P. Sylvester, P. Vermeesch, J. F. Bowring, D. J. Condon and B. Schoene, *Geostand. Geoanal. Res.*, 2016, **40**, 311–332.
29 Y. S. Zhu, J. H. Yang, J. F. Sun, J. H. Zhang and F. Y. Wu, *J. Asian Earth Sci.*, 2016, **117**, 184–207.
30 I. O. Galuskina, E. V. Galuskin, B. Lazic, T. Armbruster, P. Dzierzanowski, K. Prusik and R. Wrzalik, *Mineral. Mag.*, 2010, **74**, 365–373.
31 P. L. Zhao, S. D. Yuan, J. W. Mao, Y. B. Yuan, H. J. Zhao, D. L. Zhang and Y. Shuang, *Ore Geol. Rev.*, 2018, **95**, 1140–1160.
32 J. Mao, H. Ouyang, S. Song, M. Santosh, S. Yuan, Z. Zhou, W. Zheng, H. Liu, P. Liu, Y. Cheng and M. Chen, *Soc. Econ. Geol., Spec. Publ.*, 2019, **22**, 411–482.
33 Z. F. Zhao and Y. F. Zheng, *Am. Mineral.*, 2007, **92**, 289–308.
34 L. Ye, T. Bao, Y. P. Liu, Q. Zhang, X. J. Wang, F. Wang, D. P. Wang and J. B. Lan, *Acta Mineral. Sin.*, 2016, **36**, 503–509, (in Chinese with English abstract).
35 R. L. Romer, *Contrib. Mineral. Petrol.*, 2003, **145**, 481–491.